Journal of Solid State Electrochemistry (2019) 23:513–518
https://doi.org/10.1007/s10008-018-4158-x

ORIGINAL PAPER

Cobalt oxide thin films for high capacity and stable Li-ion battery anode

Anto P. Varghese[1] · **Shantikumar Nair**[1] · **Dhamodaran Santhanagopalan**[1]

Received: 6 August 2018 / Revised: 24 October 2018 / Accepted: 16 November 2018 / Published online: 23 November 2018

Abstract

Here, we report reactive DC-sputter deposited Co_3O_4 thin films as a promising and stable Li-ion battery anode. Thin films were deposited on stainless steel by reactive sputtering of cobalt target in O_2 atmosphere. X-ray diffraction and X-ray photo electron spectroscopy confirm the formation of Co_3O_4 crystal structure and absence of other impurities. The electron microscopy analysis shows a columnar growth morphology of the thin films while high resolution images reveal that the film is composed of ultra-small nanoparticles of average size of 5 nm. Fabricated half cells upon cycling between 3.0 and 0.01 V exhibit a stable capacity of 1125 mAh/g at a current density of 1 A/g for 100 cycles. Moreover, the electrode exhibited excellent rate capability and stability at higher rates; at current density of 10 A/g, a capacity close to 1000 mAh/g was observed. The excellent cycling stability of the cell was further confirmed by cycling at a high rate of 25 A/g (28 C) wherein the same was able to retain a capacity of 330 mAh/g even at the end of 1800 cycles. This enhanced performance could be related to the formation of 5-nm primary particles and columnar growth morphology, capable of reducing the lithium ion diffusion lengths and thus offered better kinetics even at high rates.

Keywords Anode · Co_3O_4 · DC sputtering · Li-ion battery · Thin film

Introduction

Owing to the capability to deliver higher specific capacities, transition metal oxides have attracted significant interest as lithium ion battery anodes [1, 2]. It is important to note that such transition metal oxides are useful in several energy applications including solar cells [3], supercapacitors [4], and batteries [5]. Among all, cobalt oxide particularly in cubic Co_3O_4 phase has attracted much interest due to its high theoretical capacity (890 mAh/g) and ease of synthesis [6]. Although transition metal oxides have higher theoretical capacities, they suffer from disadvantages including large initial irreversible capacity and poor cycling stability [7, 8]. However, there are several reports on improved first cycle coulombic efficiency to about 70% but at low current densities (50 or 100 mA/g) [9–12]. Similarly, compositing nanostructured Co_3O_4 with different carbon nanostructures during or post growth have also shown better rate performance [13–15]. Typically, Co_3O_4 nanostructures have reported to exhibit high specific capacity in the range of 500 to 1000 mAh/g at 1 C rate [16, 17].

Reducing electrode dimension to nanoscale is believed to be an effective approach in improving the aforementioned issues. Conventional method for electrode fabrication involves utilization of additives such as conductive carbon and binders [18]. However, these additives act as inactive mass and affect the efficient Li-ion diffusion pathways. Compared to conventional slurry casting technique, electrode films fabricated as thin films via sputter deposition have several advantages including higher energy density (additive-free, high packing density) and good electrical contact among particles and also with the current collector (adhesion) [19]. DC reactive sputtered thin film of cobalt oxide for Li-ion battery applications has never been reported, and it is important to investigate its applicability. Here, we report additive free, Co_3O_4 thin films as a promising anode for Li-ion batteries. As-obtained films were found to be smooth and uniform, consisting of particles of average particle size of 5 nm. Cells under galvanostatic cycling showed high specific capacity,

---

Electronic supplementary material The online version of this article (https://doi.org/10.1007/s10008-018-4158-x) contains supplementary material, which is available to authorized users.

✉ Dhamodaran Santhanagopalan
dsgopalan20710@aims.amrita.edu

[1] Centre for Nanosciences and Molecular Medicine, Amrita Vishwa Vidyapeetham, AIMS (P.O), Kochi 682 041, India

rate capability, and long cycling stability. At low rates (1 A/g), the electrode exhibited about 1125 mAh/g specific capacity and long cycling stability of about 1800 cycles at 25 A/g (equal to 28 C rate) delivering almost 300 mAh/g at the end.

Experimental section

All the films were deposited on stainless steel (SS316) foil which were cleaned prior to deposition. Cobalt metal target (4 in. dia, 99.99%, purchased from KJ Lesker, USA) was used for reactive sputtering with 100% O_2 as the atmosphere for deposition. The DC-chamber was pumped down to 1×10^{-6} mbar before every deposition, and the target was pre-sputtered for 5 min with argon gas to remove oxide layer on the, and the shutter remained closed throughout the pre-sputtering to prevent deposition on the loaded substrate. For cobalt oxide thin film deposition by reactive sputtering, ultra-high purity oxygen gas flow of 80 SCCM was bled in to the chamber. The sputtering power density was maintained at 1.24 W/cm^2 for 30 min. The film was deposited on a stainless steel substrate over 25 cm^2 area while before and after deposition, weight was recorded to obtain the active weight of the film per cm^2. Thin-film X-ray diffraction (Rigaku Ultimate IV, Japan) was recorded on the as-deposited film using 2θ ω geometry with continuous scan mode from 10 to 70° to understand the structural aspects, and X-ray photoelectron spectroscopy (Kratos Axis Ultra, UK) was recorded to study the surface chemistry. In order to obtain transmission electron microscopic (TEM) and high-resolution TEM images (TECHNAI G2, FEI, Germany), along with selected area electron diffraction (SAED) pattern carried out on the thin film that was prepared by scratch removing as dry powder on a copper grid by a sharp razor blade. The electrochemical cells were assembled in an Ar-filled glove box (MBraun, Germany) that is maintained with oxygen and moisture content below 1 ppm. One molar $LiPF_6$ dissolved in EC:DMC (ethylene carbonate and dimethyl carbonate) (1:1) was employed as electrolyte and lithium metal as counter electrode. Films deposited on SS-foil were used as such either as 2032 coin cells or as half-inch diameter Swagelok cells. The assembled cells were cycled in the potential window 3.0 V and 0.01 V. Galvanostatic cycling was done at different rates and long cycling stability was tested at 25 A/g.

Results and discussion

Figure 1 shows the thin-film XRD pattern of the deposited Co_3O_4 thin film. The peak observed at 44.7 corresponds to (400) plane of Co_3O_4 (JCPDS card number: 043e1003). The sharp peaks at 2θ values of 43.6° and 50.7° correspond to stainless steel which is the substrate used for deposition. TEM image displayed in Fig. 2a with rod-like features indicates a columnar growth morphology of the thin film. High-resolution transmission electron microscope (HRTEM) image shows that the thin film is composed of crystalline, uniform particles of average size of about 5 nm with lattice fringes of 0.48 nm spacing indicating (111) planes of Co_3O_4 spinel structure. Selected area electron diffraction (SAED) was further performed to study the crystal structure and shows diffused rings which could be due to the small grain size of particles. Rings indexed in the image (Fig. 2c) further confirms the spinel structure of Co_3O_4, and the (400) ring is observed to be brighter than other indexed rings complementing the XRD results of (400) oriented grains. Several TEM/HRTEM images are presented in Fig. S3 to show the columnar growth morphology and the particle size uniformity in different regions. Under the same deposition conditions, a TEM grid was directly placed in the deposition chamber (but for only 2-min deposition) for comparison (Fig. S4). The results of deposition on the grid also show ultra-small nanoparticles of about 5 nm in size which possibly indicates that the particle size is substrate independent while the columnar growth is substrate and/or thickness dependent.

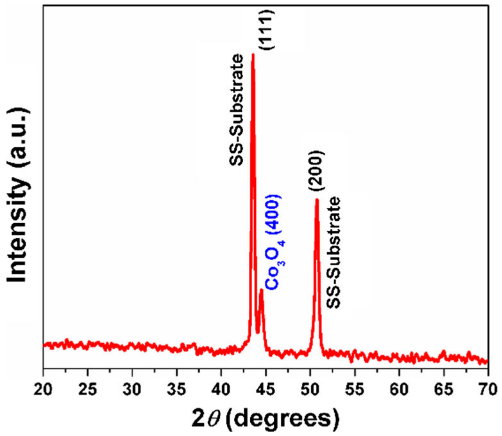

Fig. 1 XRD pattern of as-deposited thin film of Co_3O_4

Figure 3 shows the XPS profiles (survey and high-resolution spectra) of the as-deposited Co_3O_4 thin film. Spectrum was calibrated using C 1 s peak at 284.6 eV. The survey scan (Fig. 3a) shows occurrence of peaks corresponding to only oxygen, cobalt, and carbon. Absence of signals from any other elements indicates the as-deposited thin film is pure cobalt oxide. Figure 3b shows the Co 2p high resolution spectrum exhibiting two major peaks at binding energies of 795.15 eV and 780.1 eV with a spin orbital spitting of 15 eV further confirms formation of Co_3O_4. Fig. S1 shows the high - XPS spectrum of both C 1 s and O 1 s wherein the presence C-C minor peaks of C-O and C = O were present, and Co_3O_4 was confirmed by the presence of a O^{2-} peak at 529.8 eV which corresponds to the cobalt-oxygen bond. An additional peak is observed at 531.4 eV which represent the oxygen

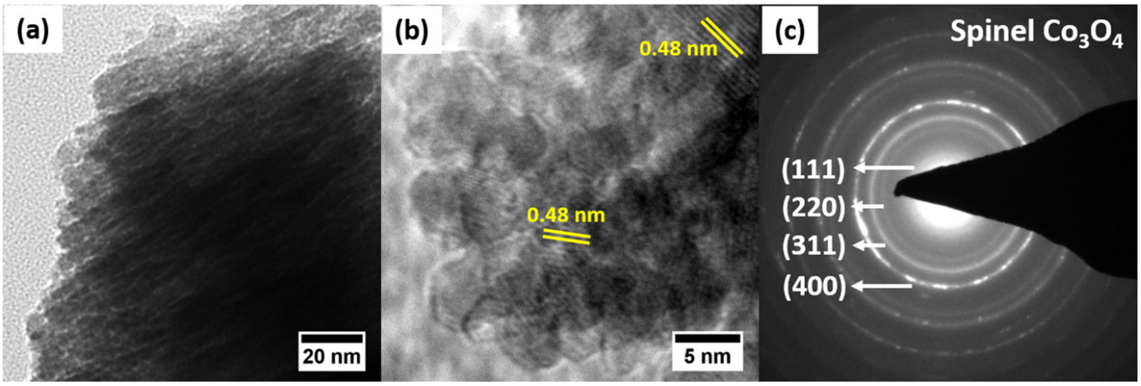

Fig. 2 **a** TEM of Co_3O_4 thin film low magnification image showing columnar growth. **b** HRTEM showing individual particles of average size of about 5 nm. **c** SAED pattern of spinel Co_3O_4 thin film showing distinct rings

species in surface-adsorbed hydroxyl ions [20]. Figure 3c shows the peak fitting for the high-resolution XPS Co $2p_{3/2}$ part of the spectrum in which Co^{2+} dominates the surface due to hydroxyl group adsorption from the atmosphere.

The first five cyclic voltammograms (CV) were investigated over a voltage range of 0.01–3.0 V at a scan rate of 0.1 mV/s (Fig. S2). First cycle shows two distinct reduction peaks at 1.42 V and 0.96 V, which corresponds to the reduction of Co_3O_4 to CoO and then to Co [21]. Two oxidation peaks are observed at 2.03 V and 1.03 V corresponding to the reversible conversion of Co to CoO and then to Co_3O_4. As reported previously, from the second cycle onwards, an occurrence of an additional reduction peak is observed at 0.7 V [22]. After CoO is reduced to Co^0, it is embedded within the Li_2O as nanograins. This process is seen to dominate as the cycle number increases. We believe that an improvement in cell capacity observed at higher rates as cycle number progresses is due to this process. There is a slight shift in the two oxidation peak shifts to 2.1 V and 1.04 V in the subsequent cycles and then stabilizes. The CV profile from second cycle onwards shows the excellent reversibility of the nanostructure.

First cycle charge/discharge profiles of the cobalt oxide film cycled at a rate of 1.0 A/g are shown in Fig. 4a. The profile is in good agreement with the first cycle of CV profile. Discharge capacity of 1700 mAh/g and charge capacity of 1200 mAh/g were recorded with about 70% coulombic efficiency. The first-cycle discharge capacity is higher than the theoretical capacity (890 mAh g^{-1}) similar to the previous reports on Co_3O_4 anodes [23, 24]. Such high capacity beyond the theoretical value is typically observed for conversion type

Fig. 3 **a** XPS spectra of as deposited thin film of Co_3O_4 survey spectra of Co_3O_4 thin film. **b** HR spectra of Co 2p. **c** Fitting of Co $2p_{3/2}$

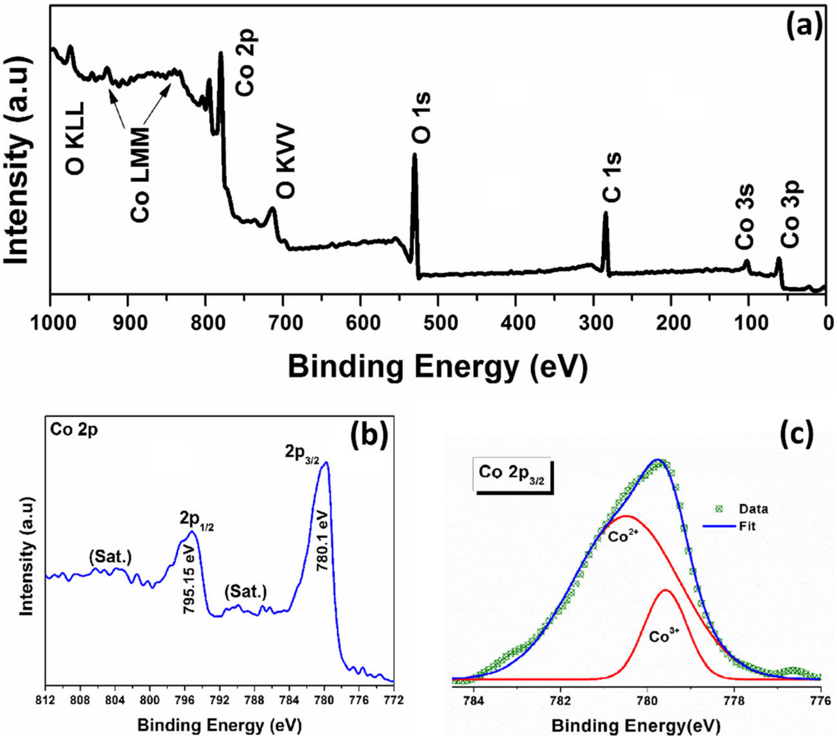

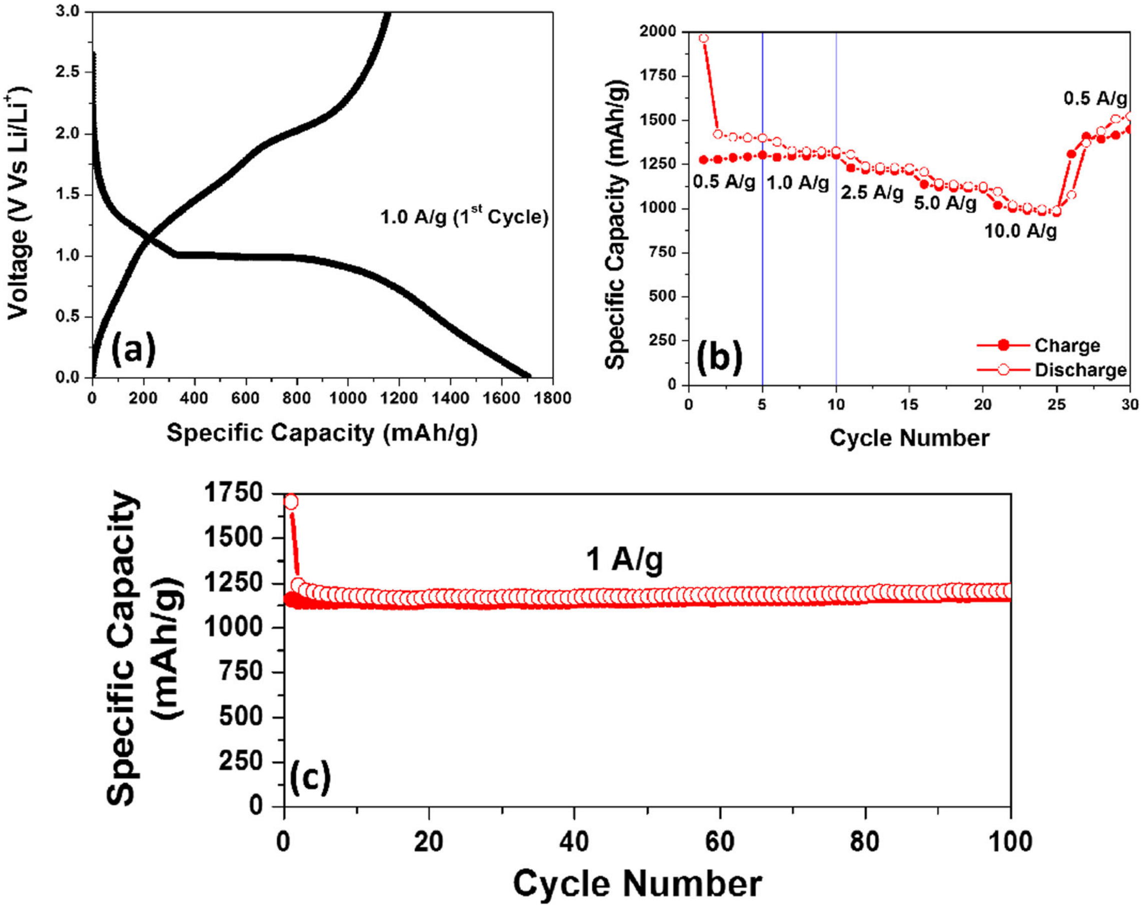

Fig. 4 **a** First cycle charge-discharge profiles of the Co_3O_4 thin film at 1 A/g. **b** Rate capability of Co_3O_4 thin film. **c** Cycling at 1 A/g for 100 cycles

anodes which is attributed to interfacial storage and the formation of reversible gel-like solid-electrolyte interface (SEI) layer [25, 26]. As presented before, our thin film consists of particles of average size of 5 nm which is possibly an ideal size range to overcome the stress due to volume expansion during lithiation/delithiation reactions. The thin film also exhibits excellent rate capability as observed from cycling at different rates (Fig. 6b) ranging from 0.5 A/g, 1.0 A/g, 2.5 A/g, 5.0 A/g, 10 A/g and back to 0.5 A/g for 5 cycles each. At higher rates (10 A/g), the cells retained a capacity close to 1000 mAh/g, and the cell regains the lost capacity when cycled back at 0.5 A/g. The specific capacity increases rapidly with subsequent cycles showing the stability of the nanostructured thin films. More than the absolute capacity values, the capacity retention of about 80% at 10 A/g compared to the capacity value obtained at 0.5 A/g is appreciable.

Figure 4c represents the long cycling performance of Co_3O_4 thin film at 1 A/g current rate. The irreversibility (~ 30%) is only observed in the first cycle and quickly improves in the subsequent cycles. Specifically, from the second cycle onwards, cell improve the coulombic efficiency and maintains > 99% in the subsequent cycles. The cell retains a capacity of 1125 mAh/g even at end of 100 cycles when cycled at the same rate pointing the excellent cycle stability of the fabricated cells. Figure 5 displays a comparison of rate-dependent specific capacities exhibited by several Co_3O_4 nanostructures reported in the literature [16, 17, 21, 27–32] with the present work. It clearly shows that the Co3O4 thin films exhibit high specific capacity even at high rates of above 10 C.

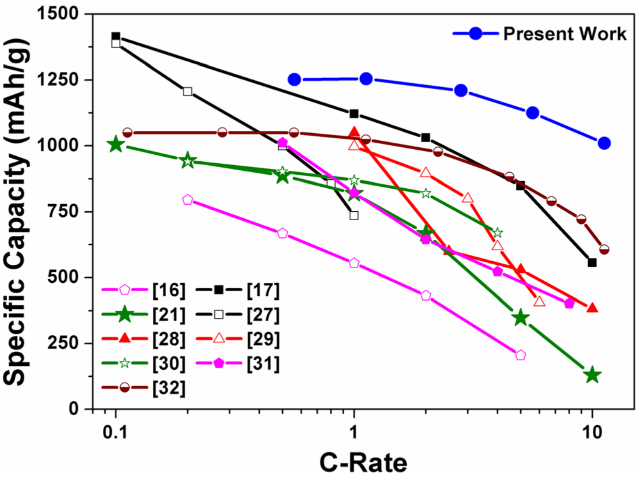

Fig. 5 Comparison of rate performance of Co_3O_4 nanostructures reported in the literature with the present work

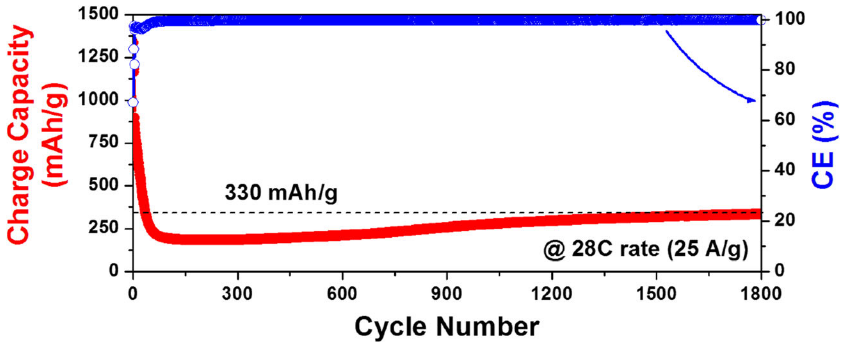

Fig. 6 Long cycling of the Co_3O_4 thin film at 25 A/g (rate equivalent to 28 C)

To extend its high rate capability, Fig. 6 shows the long cycling plot of the thin-film electrode up to 1800 cycles at a high current density of 25 A/g (equivalent to 28 C). The capacity is seen to decrease during the initial cycling which may be due to the higher current density leading to huge polarization and poor utilization of the material. Capacity was observed close to 200 mAh/g during the initial cycles but later it regains to around 330 mAh/g capacity and maintains the same till the end of 1800 cycles. The coulombic efficiency of the cells remained at 99% throughout the cycling. Such high rate capabilities (25 A/g is equivalent to 28 C) are hardly reported for Co_3O_4 nanostructures confirming the potential of reactive sputtering process for commercial applications. The columnar growth morphology and ultra-small nanoparticles are potentially responsible for the impressive performance. The Co_3O_4 thin films deposited at room temperature exhibiting high specific capacity and long cycling at high rates would be useful for solid-state Li-ion battery applications. However, the first cycle irreversibility needs to be investigated to improve the electrode performances further.

Conclusions

In summary, we reported room temperature DC-reactive sputter deposited Co_3O_4 thin films as a stable and high rate capable anode material for Li-ion battery applications. XRD and TEM/SAED analysis confirm the crystal structure to be cubic Co_3O_4, and XPS analysis further validate absence of any impurity. Electrochemical studies were performed utilizing the as-deposited thin films as electrodes in half cell configuration. The electrode demonstrated excellent long cycling performances and high rate capability. This performance emerges from columnar growth morphology and 5-nm particles interlinked that is capable of shortening the diffusion length and thus enhanced the kinetics. The electrode even demonstrated high rate (28 C) and long cycling performances (1800 cycles). The first cycle irreversibility is still an issue and needs to be further investigated. However, the fact that the electrodes retain a high capacity after 100 cycles makes this a promising anode and can be utilized as a candidate for solid state battery applications.

Acknowledgements DS acknowledges Science and Engineering Research Board, India for awarding of Ramanujan Fellowship (Ref: SB/S2/RJN-100/2014). The PVD cluster deposition system funded by Amrita is greatfully acknowledged. APV acknowledges financial support from Department of Science and Technology, India (SR/NM/PG-01/2015).

References

1. Wang X, Li X, Sun X, Li F, Liu Q, Wang Q, He D (2011) Nanostructured NiO electrode for high rate Li-ion batteries. J Mater Chem 21(11):3571–3573
2. Wang L, Xu HW, Chen PC, Zhang DW, Ding CX, Chen CH (2009) Electrostatic spray deposition of porous Fe_2O_3 thin films as anode material with improved electrochemical performance for lithium-ion batteries. J Power Sources 193(2):846–850
3. Lan Z, Que L, Wu W, Wu J (2015) Preparation of Pt-NiO/Co_3O_4 nanocompounds based counter electrodes from Pt-Ni/Co alloys for high efficient dye-sensitized solar cells. J Alloys Compd 646:80–85
4. Zhang J, Lin J, Wu J, Xu R, Lai M, Gong C, Chen X, Zhou P (2016) Excellent electrochemical performance hierarchical Co_3O_4@Ni_3S_2 core/shell nanowire arrays for asymmetric supercapacitors. Electrochim Acta 207:87–96
5. Jena A, Munichandraiah N, Shivashankara SA (2015) Metal-organic chemical vapor-deposited cobalt oxide films as negative electrodes for thin film Li-ion battery. J Power Sources 277:198–204
6. Donders ME, Knoops HCM, Kessels WMM, Notten PHL (2012) Co_3O_4 as anode material for thin film micro-batteries prepared by remote plasma atomic layer deposition. J Power Sources 203:72–77
7. Zhou G, Wang DW, Li F, Zhang L, Li N, Wu ZS, Wen L, Lu GQ(M), Cheng HM (2010) Graphene-wrapped Fe_3O_4anode material with improved reversible capacity and cyclic stability for lithium ion batteries. Chem Mater 22(18):5306–5313
8. Kim S-J, Kim E-J, Liu M, Shin H-C (2016) Cobalt oxide nanorods prepared by a template-free method for lithium battery application. J Electrochem Sci Technol 7(3):206–213
9. Zhan L, Wang Y, Qiao W et al (2012) Co_3O_4 nanocages for high-performance anode material in lithium-ion batteries. J Phys Chem C 116:7227–7235
10. Sun Y, Feng XY, Chen CH (2011) Hollow Co_3O_4 thin films as high performance anodes for lithium-ion batteries. J Power Sources 196(2):784–787
11. Huang H, Zhu W, Tao X, Xia Y, Yu Z, Fang J, Gan Y, Zhang W (2012) Nanocrystal-constructed mesoporous single-crystalline

Co_3O_4 nanobelts with superior rate capability for advanced lithium-ion batteries. ACS Appl Mater Interfaces 4(11):5974–5980

12. Yan C, Chen G, Zhou X, Sun J, Lv C (2016) Template-based engineering of carbon-doped Co_3O_4 hollow nanofibers as anode materials for lithium-ion batteries. Adv Funct Mater 26(9):1428–1436
13. Pan A, Wang Y, Xu W, Nie Z, Liang S, Nie Z, Wang C, Cao G, Zhang JG (2014) High-performance anode based on porous Co_3O_4 nanodiscs. J Power Sources 255:125–129
14. Lu Y, Wang Y, Zou Y, Jiao Z, Zhao B, He Y, Wu M (2010) Macroporous Co_3O_4 platelets with excellent rate capability as anodes for lithium ion batteries. Electrochem Commun 12(1):101–105
15. Kim H, Seo DH, Kim SW, Kim J, Kang K (2011) Highly reversible Co_3O_4/graphene hybrid anode for lithium rechargeable batteries. Carbon N Y 49(1):326–332
16. Li B, Cao H, Shao J, Li G, Qu M, Yin G (2011) Co_3O_4@graphene composites as anode materials for high-performance lithium ion batteries. Inorg Chem 50(5):1628–1632
17. Leng X, Wei S, Jiang Z, Lian J, Wang G, Jiang Q (2015) Carbon-encapsulated Co3O4 nanoparticles as anode materials with super lithium storage performance. Sci Rep 5(1):16629
18. Wang H, Mao N, Shi J, Wang Q, Yu W, Wang X (2015) Cobalt oxide-carbon nanosheet nanoarchitecture as an anode for high-performance lithium-ion battery. ACS Appl Mater Interfaces 7(4):2882–2890
19. Liao CL, Lee HY, Chang ST, Fung KZ (2006) Structural characterization and electrochemical properties of RF-sputtered nanocrystalline Co3O4 thin-film anode. J Power Sources 158(2):1379–1385
20. Wang L, Liu B, Ran S, Huang H, Wang X, Liang B, Chen D, Shen G (2012) Nanorod-assembled Co_3O_4 hexapods with enhanced electrochemical performance for lithium-ion batteries. J Mater Chem 22(44):23541
21. Huang G, Xu S, Lu S, Li L, Sun H (2014) Micro-/nanostructured Co_3O_4 anode with enhanced rate capability for lithium-ion batteries. ACS Appl Mater Interfaces 6(10):7236–7243
22. Zhou X, Shi J, Liu Y, Su Q, Zhang J, du G (2014) Microwave irradiation synthesis of Co_3O_4 quantum dots/graphene composite as anode materials for Li-ion battery. Electrochim Acta 143:175–179
23. Tan Y, Gao Q, Yang C, Yang K, Tian W, Zhu L (2015) One-dimensional porous nanofibers of Co_3O_4 on the carbon matrix from human hair with superior lithium ion storage performance. Sci Rep 5(1):12382
24. Liu HC, Yen SK (2007) Characterization of electrolytic Co_3O_4 thin films as anodes for lithium-ion batteries. J Power Sources 166(2):478–484
25. Binitha G, Ashish AG, Ramasubramonian D, Manikandan P, Shaijumon MM (2016) Lithium-ion batteries: 3D interconnected networks of graphene and flower-like cobalt oxide microstructures with improved Lithium storage. Adv Mater Interfaces 3(1):1500419
26. Keppeler M, Srinivasan M (2017) Interfacial phenomena/capacities beyond conversion reaction occurring in nano-sized transition-metal-oxide-based negative electrodes in lithium-ion batteries: a review. ChemElectroChem 4(11):2727–2754
27. Wang R, Xu C, Sun J, Liu Y, Gao L, Lin C (2013) Free-standing and binder-free lithium-ion electrodes based on robust layered assembly of graphene and Co_3O_4 nanosheets. Nanoscale 5(15):6960–6967
28. Wang Y, Zhang HJ, Lu L, Stubbs LP, Wong CC, Lin J (2010) Designed functional systems from peapod-like Co@carbon to Co_3O_4@carbon nanocomposites. ACS Nano 4(8):4753–4761
29. Xing L, Chen Z, Xue X (2014) Controllable synthesis Co_3O_4 nanorods and nanobelts and their excellent lithium storage performance. Solid State Sci 32:88–93
30. Zheng J, Zhang B (2014) Facile chemical bath deposition of Co_3O_4 nanowires on nickel foam directly as conductive agent- and binder-free anode for lithium ion batteries. Ceram Int 40(7):11377–11380
31. Mo Y, Ru Q, Song X, Hu S, An B (2014) A novel dendritic crystal Co_3O_4 as high-performance anode materials for lithium-ion batteries. J Appl Electrochem 44(7):781–788
32. Li Z, Yu X-Y, Paik U (2016) Facile preparation of porous Co_3O_4 nanosheets for high-performance lithium ion batteries and oxygen evolution reaction. J Power Sources 310:41–46